Computational Biology and Bioinformatics
2015; 3(2): 31-39
Published online April 27, 2015 (http://www.sciencepublishinggroup.com/j/cbb)
doi: 10.11648/j.cbb.20150302.12
ISSN: 2330-8265 (Print); ISSN: 2330-8281 (Online)

Dynamics of βB2-Crystallin Motion Based on Principal Component Analysis and Normal Mode Analysis

Alaa El-Din A. Gawad

Biophysics and Laser Science Unit, Research Institute of Ophthalmology, Giza, Egypt

Email address:
alaael_din3@hotmail.com

To cite this article:
Alaa El-Din A. Gawad. Dynamics of βB2-Crystallin Motion Based on Principal Component Analysis and Normal Mode Analysis. *Computational Biology and Bioinformatics*. Vol. 3, No. 2, 2015, pp. 31-39. doi: 10.11648/j.cbb.20150302.12

Abstract: The primary function of lens is to focus images perfectly on the retina. Lens crystallins however are flexible nanomachines that frequently accomplish their biological function by collective atomic motions in and/or out the lens. Although genetic and biochemical data on the βB2-crystallin protein are available from several sources, the correlation between conformational changes and dynamic behavior at the atomic level remains to be understood. The βB2-crystallin dimer has studied through a combination of molecular dynamics simulations, principal component analysis (PCA) and normal mode analyses. The changes in interface buried surface shows the mutual orientation of individual domains in βB2-crystallin dimer. The dominant PCA modes for concerted motions of the protein atoms were monitored in a lower-dimensions subspace. Three types of movements found in βB2-crystallin dimer, which are a twist propeller motion, a scissors type hinge motion, and a shear motion between the domains. Both the RMSF and the normal-mode dynamics showed that N-terminal β-sheet is the most correlated segments.

Keywords: Conformational Change, Essential Dynamics, Normal Mode Analysis, Elastic Network Model, Molecular Dynamics, B-Crystallin

1. Introduction

The collective motion is used as a synonym of any kind of specific motion pattern of individual units. This dynamic behavior of proteins is the key for their functions; namely, the predisposition of the proteins to undergo conformational transitions is usually activated process characterized by large amplitude, harmonic low-frequency motions [1-3]. The collective motion is involved in numerous biological processes including enzyme catalysis, channel gating, allosteric interactions, signal transduction, and recognition dynamics. The observed motions of the protein conformational changes can be used to investigate the conformational energy landscape, to improve sampling efficiency and in the refinement of X-ray and NMR data [4, 5].

Lens transparency depends on the accurate delineation of the prominent structure of crystallins and their short-range arrangement in lens fibers [6]. These proteins, however, could occupy different microstates or subsets of conformation that coexist in dynamic equilibrium with maintaining the capability of passing light without scattering. β-Crystallins are about 45% of total lens proteins [7, 8]. They are oligomers formed from a wide variety of subunits. It adopts different sizes of aggregates, depending on protein concentration, pH, and ionic strength [9, 10]. β-Crystallins have β-strands, which fold into two domains of roughly equal size: the N terminal domain (NTD), and the C terminal domain (CTD) (Figure 1) [11]. All β-crystallins have N-terminal extensions, while basic β-crystallins also have C-terminal extensions. The two domains are connected via a short extended helix peptide that forms an interdomain hinge region [12, 13]. βB2-Crystallin is the major β-crystallin subunit, comprising approximately 40% of the total β-crystallin aggregates and, in solution, isolated βB2 exists as dimers [14]. Moreover, βB2-crystallin subunits that lacking both N-terminal and C-terminal extensions can also assemble into dimers [15, 16]. It has been reported that peptide linker in βB2-crystallin is necessary for dimerization [16]. βB2-Crystallin is not essential for the normal development of a transparent lens in the mouse. It plays an increasingly important role in maintaining the transparency of the lens after birth, possibly by interacting with other crystallins to increase their resistance to thermal denaturation and oxidative stress [17].

Normal mode analysis (NMA) has been extensively applied to determine protein slow motions, which are coupled to

vibrational and thermal fluctuations [18]. The NMA method predicts all possible deformations a protein can undergo around its native state by representing the protein by a set of harmonic oscillators [19, 20].

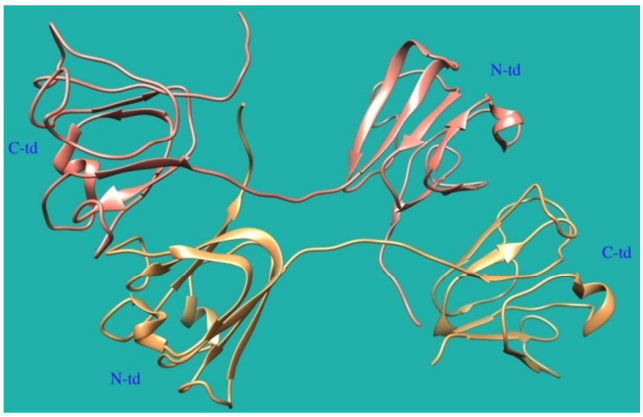

Figure 1. *A dimer of βB2-crystallin structure. Diagrammatic representation of subunit A structure (goldenrod color) and subunit B structure (salmon color).*

In the elastic network model (ENM) a protein structure is represented by a linear elastic network (EN) in which each node is the Cα atom of a residue and the all-atoms molecular mechanics force-field is replaced by a ball and spring harmonic (Hookean) potential, combined with a coarse grained (CG) representation of the protein. There are various ENM model types of coarse-grained normal mode analyses [2, 21, 22]. Among these models, anisotropic normal mode model (ANM) is a simple physics-based model that use the 3N mass-weighted coordinates of the nodes as generalized coordinates, which exclusively depends on inter-residue contact topology that can be described by a matrix version of Newton's second law of motion (quadratic potential) with a uniform force constant for all atomic interactions within a cutoff distance reproduced almost identically the low-frequency modes of motion obtained with a detailed force field [23, 24]. ANM method has been successfully applied for exploring the relation between function and dynamics in several cases, e.g. lysozyme [25] and influenza virus hemagglutinin [26], nicotinic acetylcholine receptor transmembrane domain [27], microtubules [28], and p38 MAP kinases [29].

The principal components analysis (PCA) is a simple way to reduce the dimension of complex datasets. The main goal of PCA is to reduce the phase space of original representation of protein motion into a lower dimensional representation that captures the dominant modes of motions of the protein. PCA has been used in a wide range of biomedical problems, including the analysis of an ensemble of conformations, typically derived from MD simulations as well as the analysis of a large set of experimental structures [30-32].

The aim of the present study is to provide much detailed information about the motions of βB2-crystallin dimer to understand its conformational changes which are important for its functions.

2. Material and Methods

2.1. Molecular Dynamics Simulation of Protein

The initial structure of the βB2-crystallin was retrieved from the Protein Data Bank, entry 1BLB (X-ray, 3.30 Å resolution). The molecular simulation was conducted to the dimer structure A and B subunits of βB2-crystallin coordinate contained in the asymmetric unit of the native tetramer structure. The molecular dynamics package Amber suite 12 [33] with the ff99SB force field was utilized to perform MD simulations of the βB2-crystallin monomer in explicit solvent. The βB2-crystallin structure was taken from the protein data bank [12]. The βB2-crystallin were immersed in a 12,450 TIP3P water box of 63.312 Å X 81.320 Å X 105.320 Å size, resulting in a system with total number of 43123 atoms. Only five Na+ ions were added using XLEAP in AMBER 12 suite, corresponding to the minimum number of counterions necessary to neutralize the system. Periodic boundary conditions and particle-mesh Ewald [34] treatment of the electrostatics were employed. A cutoff of 8 Å was used for Lennard-Jones interactions and SHAKE [35] to constrain all covalent bonds involving hydrogen. The minimization procedure started with 1000 steepest descent steps followed by about 2000 steps of conjugate gradient. Subsequently, the solvated system was equilibrated for 100 ps at constant volume and temperature (T = 298 K) using the Berendsen coupling procedure [36] with position restraints on protein backbone. The system was then equilibrated further at isothermal–isobaric ensemble for 5ns. The temperature and pressure coupling parameters were set as 2 ps. Production run was then performed in NPT ensemble at 298 K for 10 ns and configurations were saved every 10 ps.

Trajectory analyses, including RMSF and RMSD were performed using PTRAJ module. This module was then used to perform principal component analysis (PCA) on the MD trajectories.

2.2. Principal Component Analysis

Protein simulation is aiming at generating enough configurations of the system of interest to extract functionally relevant motions. PCA method has been very popular to reduce the generated dimensionality of MD trajectory to an essential subspace encompassing few degrees of freedom, eliminating the positional fluctuations. PCA technique is commonly used to extracts the concerted motion in simulations that are essentially correlated and presumably meaningful for biological function [37]. In the PCA analysis, mass-weighted covariance matrix (C) was constructed from the trajectories. The input is an n by p coordinate matrix X where n is the number of structures and p is 3 times the number of residues [38]. Each row in X represents the C_α coordinates of each structure. From X the elements of the covariance matrix C are calculated as

$$C = \langle (xi - \langle xi \rangle)(xi - \langle xi \rangle) \rangle$$

where averages over the n structures are indicated by the

brackets ‹›. The covariance matrix *C* can be decomposed as

$$C = P\Delta P^T$$

Where the eigenvectors *P* represent the principal components (PCs) and the eigenvalues are the elements of the diagonal matrix Δ. The eigenvalues represent the amplitude of the eigenvectors along the multidimensional space, and the displacements of atoms along each eigenvector showed the concerted motions of protein along each direction. Prior to performing PCA, all translations and rotational motions were eliminated by fitting the trajectory to a reference structure, in this case, the minimized structure.

2.3. Anisotropic Normal Mode (ANM) Analysis

Normal mode analysis was applied to the crystal structure of βB2-crystallin. ANM calculations were done using the Anisotropic Network Model web server [39]. The model assumes that all C_α atoms within a specified cut-off distance are attached by uniform springs. The equilibrium distance between the atoms is then determined from the initial structure. All runs were performed online at http://ignmtest.ccbb.pitt.edu/cgi-bin/anm/. Each analysis used a distance cutoff of 15 Å and a weighted C–C distance of 2.5 Å.

2.4. Graphical Representation

Graphical views and movies of the models were performed with PyMoland Modevectors.py.

3. Results

3.1. Molecular Dynamics Simulation

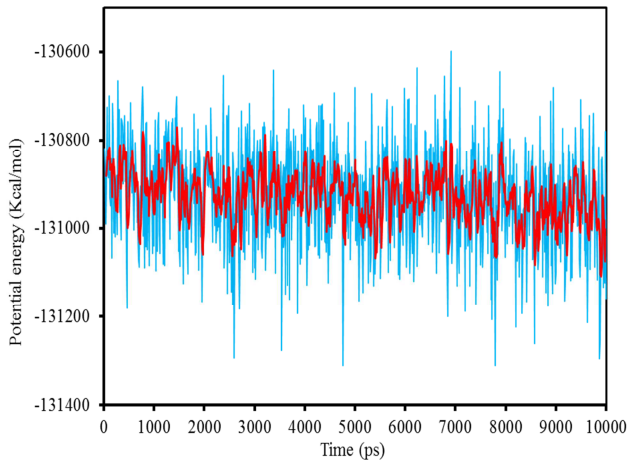

Figure 2. *Potential energy of the βB2-crystallin as a function of time during MD. The solid red line is a running average over 5 ps.*

The dimeric form of βB2-crystallin represents the minimal oligomeric unit, thus, in setting up this simulation, two of the subunits omitted of the tetramer subunits from the crystal structure of the βB2-crystallin (PDB entry 1BLB) [13]. Molecular dynamics of βB2-crystallin dimer was performed as described in Methods. The stabilities of the βB2-crystallin dimer (366 residues) observed during the MD simulation were determined by two criteria to assess whether the simulation achieved equilibrium or steady-state sampling. The first is the conservation of energy and maintenance of a constant average temperature. In my case, molecular dynamics simulation study revealed a consistent value of the energy of the molecule throughout the time period of simulation, which is an indication of strong basis of the fact that the molecule has a stable structure (Figure 2).

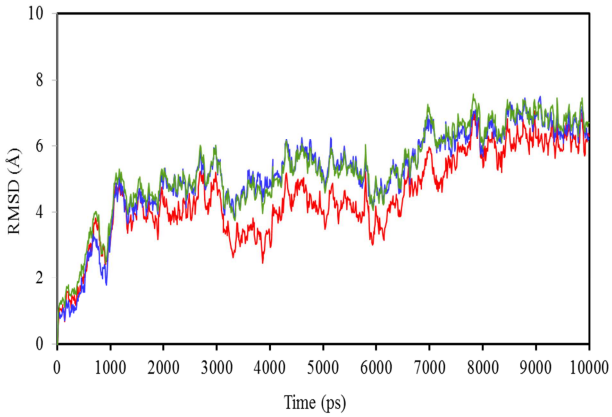

Figure 3. *RMSD values of Cα from the initial structures. Green line indicates RMSD values of the dimer and red and blue lines indicate RMSD values of the two subunits (A & B) respectively.*

To assess further the conformational stability of the βB2-crystallin dimer during the MD simulation, the time-dependent the root-mean-square deviation (RMSD) of the Cα atoms with respect to the corresponding initial structures was calculated. Figure (3) shows an initial drift in RMSD which may be due to the difference of crystal structure with solution structure. There also are few differences in the Cα RMSD values for each dimeric subunit. It is evident from figure (3) that the Cα RMSD values for both the dimer and the subunit B remained almost the same during the whole simulation time (10 ns), although the subunit A deviated from the initial structure less than the dimer. These structures undergo large conformational change over the course of the simulation, with the root main square deviation in Cα atom positions from the starting structure peaking at >6 Å at ≈8.5 ns. The results suggest the presence of two apparent substates, one existing from about 1500 to 4100 ps and the other one from about 4100 ps to 10,000 ps. The individual subunits, however, are quite stable, with an average RMSD of <8.0Å, indicating that this conformational change is mainly due to the rigid body motions of the individual subunits relative to one another. However, more detailed meticulous studies must be carried out to investigate this behavior.

The flexibility of different segments of the protein is revealed by looking at the root mean square fluctuation (RMSF) of each residue from its time-averaged position. RMSF of Cα is presented as a function of residue number in figure (4). From RMSF, the two subunits display a similar fluctuation pattern.it is evident that a large part of residues in subunit A and subunit B are characterized by fluctuations not

higher than 3.0 Å, apart from the first 4 amino acid residues in the N-terminal arm of subunit A reaches 7Å (data not shown). Interestingly pronounced fluctuations are observed for residue P21 and T91-N95 in subunit A than subunit B.

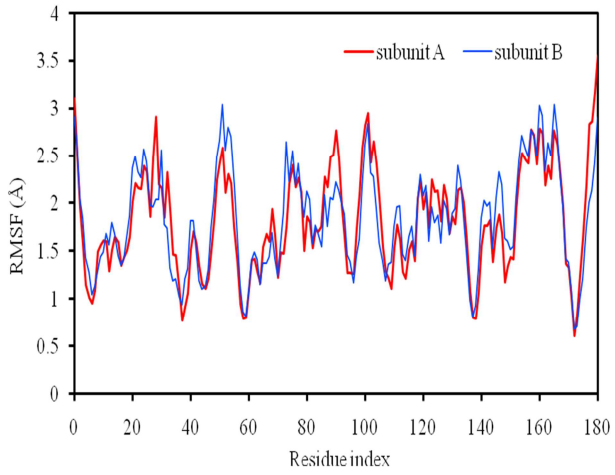

Figure 4. *Calculation of Cα-RMSF for each subunit was performed, based on superposition using Cα best fits for its own subunit.*

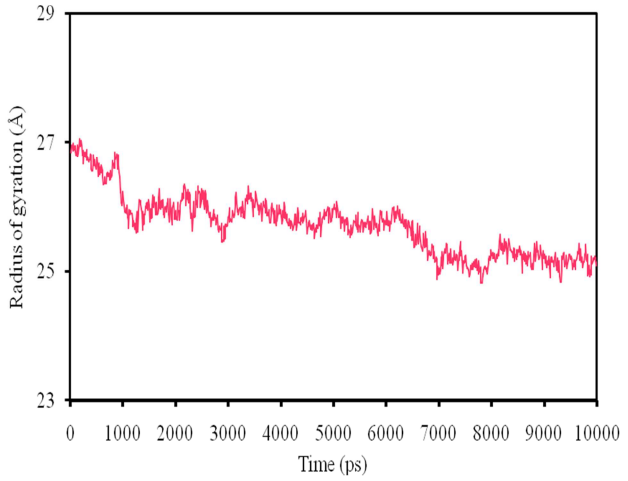

Figure 5. *The plot of gyration radius of dimeric protein in explicit water box.*

Over the course of the MD simulation, the radius of gyration (Rg) parameter was further evaluated, and it was observed that initially the radius of gyration fluctuated around the initial X-ray Rg value during the first 800 ps (Figure 5). The Rg value for the whole protein dimer was then decreased from ~26.7 Å to a value of 25.78 Å after 1100 ps of the MD simulations. The radii of gyration after 6100 ps of the MD simulations demonstrated the same tendency to more compact structures with Rg value of 25.1Å. Thus, the comparison of the radii of gyration during the 10 ns MD simulations suggests that the protein dimer promotes the extended conformations and then contract with decreasing radius of gyration.

The conformational perturbation of the crystallographic dimer observed at interfacial region during the 10 ns simulations of the βB2-crystallin dimer with respect to the starting structure was further characterized with the DynDom program [40]. DynDom identifies rigid domains on the basis of their differing rotational properties, and in addition it identifies the hinge axis and the corresponding hinge bending residues from two protein structures that have different conformations. DynDom analysis reports that the subunit A and subunit B rotate a 44.2° and 42.5° respectively when both are superimposed on to its initial structure. The Protein Interfaces, Surfaces and Assemblies (PISA) server was used to further analyze complex interfaces [41]. Such relative rotation of two subunits also causes the buried interaction surface between the subunit A and subunit B to become 3059.0 Å. PISA (http://www.ebi.ac.uk/pdbe/pisa/) analysis of protein interface present in the crystal also suggested that the size of the buried surface area formed is 3869.4 Å.

3.2. Principal Component Analysis

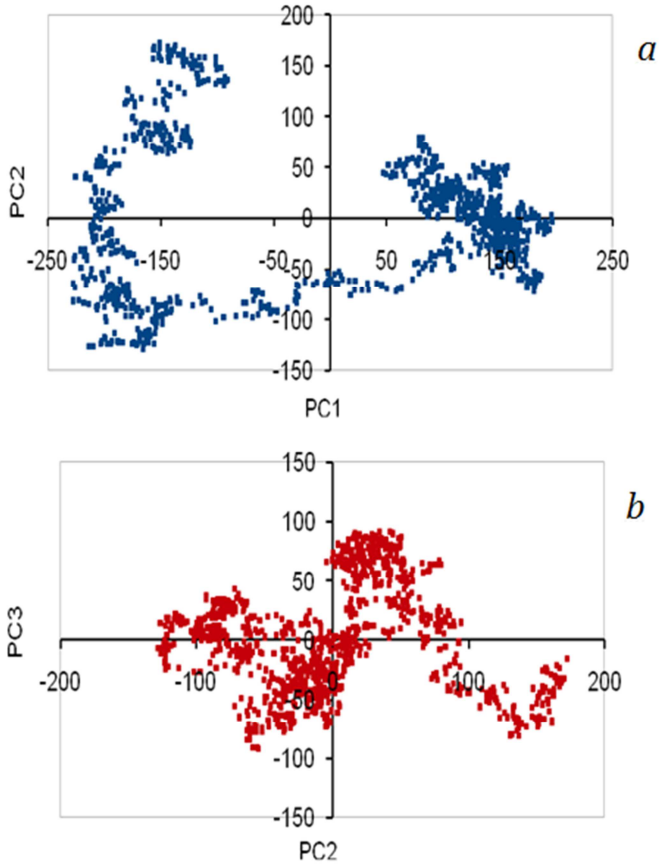

Figure 6. *projections of individual structures along pairs of the first three principal component directions for bovine βB2-crystallin simulation (10ns).*

The PCA was conducted to molecular dynamics trajectories to examine major conformational changes between the structures and map them onto a lower phase subspace. The lowest mode shapes computed using PCA, are projected onto the energy-minimized structures of βB2 dimer. One can see undoubtly that the molecule undergoes sharp conformational transitions, indicative of jumps between multiple isomeric states. This multimodality suggests that the MD simulation spends much of the run time in a few basins. It is evident from figure (6a) that PC1 varies more broadly compared to PC2. This corroborates well to the eigenvalue distribution plot

where PC1 has the highest eigenvalue (data not shown). The 2-D projections have been appeared to have more converged pattern for βB2-crystallin dimer. Interestingly, the PC3 is focusing near the origin of the plot (figure 6b).

3.3. Normal Mode Analysis of A Coarse-Grained Model

To explore the conformational dynamics of βB2-crystallin dimer, a more coarse-grained model of the protein motions (normal-mode analysis) was carried out for the crystal structure. In other words, the ANM analysis is performed for a single structure, not an ensemble. The model assumes that all Cα atoms within a specified cut-off distance are attached by uniform springs with typical force constant of 6.0 pN.nm/Å2. The topology of the protein along with the cut-off distance and spring constant specify the potential energy of the system and the subsequent dynamics. In the present set of calculations, a uniform spring constant was used and a cut-off distance of 15 Å.ANM predicts the directionalities of the collective motions in addition to their magnitudes. As usual, the first six modes correspond to eigenvectors with zero eigenvalues (i.e., translations and rotations), are discarded; and the representative motions related to the top-rank modes 7, 9, 14, 15, and 18 were depicted in Figure 7. Mode-7 described the hinge bending motion of the protein dimer with substantial fluctuations around residues Q86 to H88 (Figure 7a). In this mode, there is also significant motion between the residues 108-110 of β-strand c3 and the residues 122-130 of β-strand d3. Mode-9 showed a concerted rotation of the N-terminal domain of subunit A with respect to C-terminal domain of subunit B and vice versa (Mode-18). In these models, the motion bisects each domain motion into clockwise (motifs 3 & 4) and anticlockwise (motifs 1 & 2) swing (Figure 7b & 7e). This motion triggers the fluctuation of residues in b1, c1, and d1 β-strands and 310 helical region and d2 β- strand in subunit A and b3 β-strand and 310-helix in the C-terminal of subunit B. In mode-18 (Figure 7e), the linker between b3 and c3, the linker between a4 and b4 and 310-hlix of the N-terminal domain undergoes fluctuation. It is worthy of note that modes 14 and 15 give rise to twisting motion of N-terminal domain of subunit A and C-terminal domain of subunit B for earlier and vice versa for later (Figure 7c). These modes described a large flexibility of G-13 and linker between c1 and d1 B-strands in N-terminal domain and linker between a3 and b3 strands. The residues Q161-P162 of d3 strand showed high flexibility of C-terminal of subunit A. In subunit B, the residues composing left-handed α-helix, 310-helix and linker between c3 and d3 of C-terminal domain are flexible. While the residues D66-S67 of 310-helix of N-terminal domain between c2 and d2 are much less flexible (Figure 7d).

The overlap between molecular dynamics simulation data and the ANM modes is calculated to detect any correlation between the motions of the experimental structure (MD simulation) and the slow modes. The top-rank three ANM modes were found to yield the highest correlation (among all ANM modes) with PC1, PC2, and PC3 respectively (data not shown). It has been found that a significant overlap between those conformations sampled by unconstrained MD and those determined in order to satisfy NM constraints. There is a very strong overlap between the distributions of the second and third PC and second and third NM, which is strong evidence that these are components of the same mode.

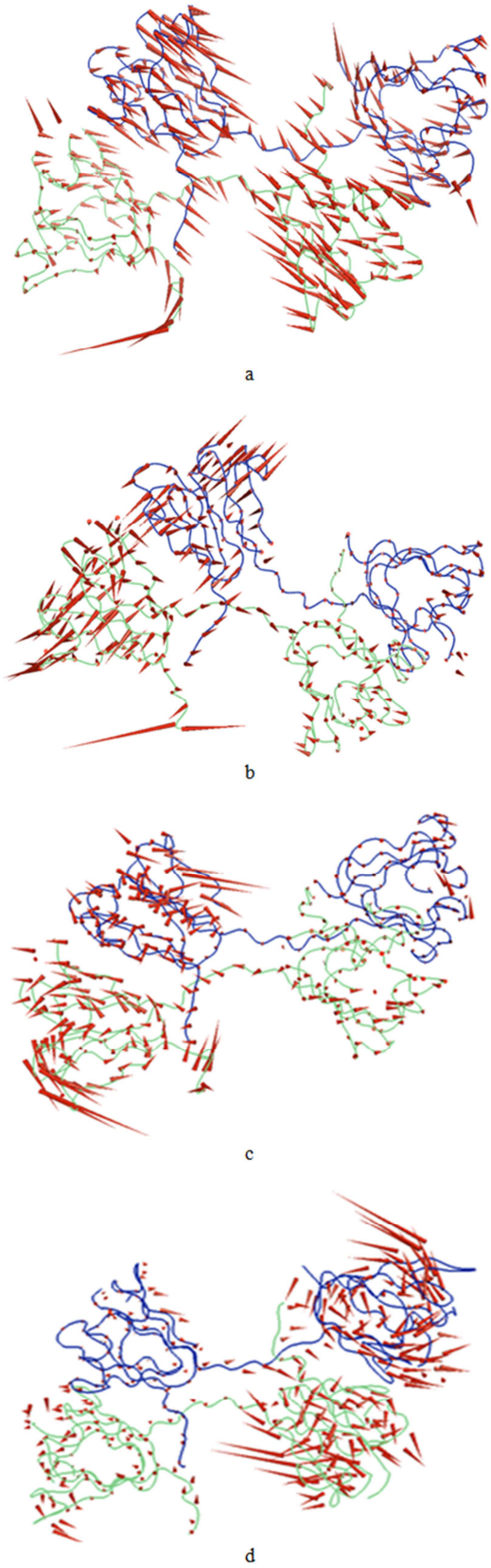

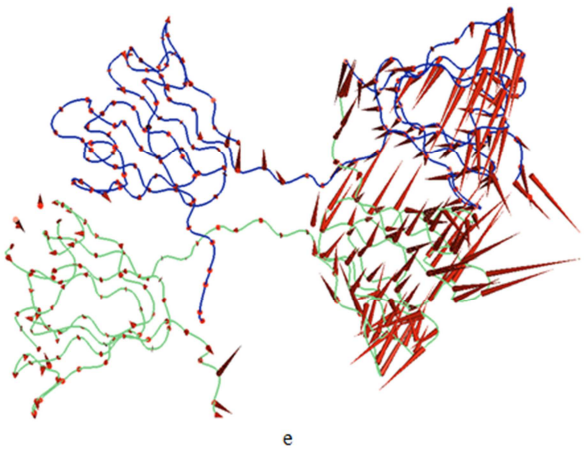

Figure 7. *Porcupine (red cones) representation of the direction of motion observed along the representative lowest-frequency normal modes 7, 9, 14, 15, and 18 acquired from ANM analysis.*

3.4. Dynamic Cross Correlation Analysis

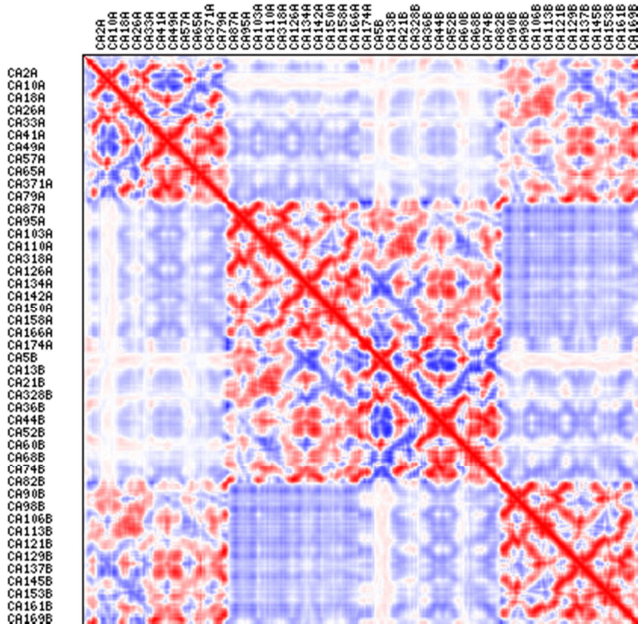

Figure 8. *Correlation map calculated with only the lowest frequency modes revealing correlated and anti-correlated regions in the protein structure.*

Correlations between residue fluctuations describe the relations between the displacements of different parts of the protein, i.e. the structure that move collectively, as a unified group, and how these regions move with respect to one another. The cross-correlation matrix from the normal modes of the βB2-crystallin was depicted in (*Figure 8*) where the axes represent the sequences for βB2-crystallin dimer. Blue and red colors in this map indicate negatively (opposite direction) and positively (same direction) correlated regions, respectively. The colors in the map indicate different strengths and types of inter-residue orientational correlation functions. Both the N-terminal domain (residues 2-81) and C-terminal domain (residues 87-175) which cover the core protein show negatively correlated motions with respect to each other. So this suggests that these two domains make motions in opposite directions. The two domains are characterized by a flexible extended interdomain. Of interest, region of the connecting peptide, including V83, D84, S85, Q86, E87 and H88 of the linker region and a3 β-strand of motif-3 of C-terminal domain show significant correlated motions. The cd long arch in N-terminal domain show strong correlated motion with K89 and I90 residues of a3 β-strand of motif-3. Moreover, it is observed that d3 β-strand motif and b4 β-strand of motif-4 rotate in opposite directions.

4. Discussion

An understanding of the conformational changes involved in the function of lens crystallins is of great interest. Furthermore, lens crystallins are also nanomachines undergo large conformational changes to carry out their biological (lenticular) function [42, 43]. Cataractogenesis is a downstream process emerging from loss of solubility and/or stability of crystallins [44-46]. However, the cataract pathology was unlikely to be associated with a direct folding defect [47]. Collective motions suggest that flexibility and internal motions are important for many protein functions [48-50]. Principal component analysis (PCA) and normal mode analysis (NMA) are invaluable tools for studying conformational changes in proteins. βB2-Crystallin forms dimers, tetramers and oligomers by changing the conformation of the linker and allow domain to swap partners between two molecules [51, 52]. The MD simulation suggests that the internal structures of the βB2-crystallin domains do change much at normal temperature (Figure 2).

To address the question whether this is simply unfolding process in the simulations or is due to the motion of subunits in the homodimer. The all backbone atoms of motif 1 of N-terminal domain from X-ray crystallographyare known to be disordered in the subunit A. However, during MD simulation (10 ns) this motif folds into its native-like beta-sheet structure. This folding behavior is accompanied by sliding of the subunits. However, the molecular dynamics simulation of N-terminal domain showed little variations compared to the initial wild-type crystal structure at room temperature (PDB code, 1E7N; 53). Moreover, βB2-crystallin domains show similar amplitudes of the internal motions (Figure 4). It has been reported that calf βB2-crystallin remains soluble following incubation at temperatures up to 90°C [54]. More recently, the solvent accessibility studies of βB2-crystallin demonstrated that the C-terminal domain is considerably more stable than N-terminal domain. Furthermore, differences in initial levels of deuterium incorporation between the N- and C-terminal domains suggested a more highly accessible N-terminal domain and a more compact C-terminal domain [55].

The trajectory along the first PCs determined in the run MD is carried out on subsets of the protein atoms such as Cα atoms only (10 ns, Figure 6). One can see unambiguously that the molecule undergoes sharp conformational transitions, indicative of jumps between two or three isomeric states. Noteworthy, principal component analysis of a molecular

dynamics simulation suffices to drive conformational subspace by the relatively short time scale of the order of few nanoseconds [56, 57]. MacDonald et al., (2005) [53] has reported that explicit-solvent molecular dynamics simulation of the N-terminal domain of rodent βB2-crystallin at 500 K showed local flexibility of β-hairpin cysteine. Moreover, principal component analysis of wild type protein shows conformationally variable local patterns of alterations in the N-terminal domain.

Normal mode analyses are of particular interest because they demonstrate that protein function is determined by protein motions more directly than by protein structure. The robustness of the proposed approach for modeling flexibility has been tested in diverse contexts [58-60]. β/γ-Crystallin superfamily has a tertiary structure composed of four Greek-key motifs divided into two globular β-sheet domains. Analyzing the motion of βB2-crystallin revealed anisotropic domain motions (Figure 7). It has been reported that the low-frequency modes of any macromolecule are highly anisotropic [61]. Moreover, the most relevant vibrational motions in β-sheets are twisting and bending with respect to an in-plane axis perpendicular to the β-strands [62]. It has been reported that the regions of slowest solvent accessibility in βB2 dimer were found in residues 121-164 of the core of the C-terminal domain, including the buried interface peptides. The truncation of the last three beta sheets in the C-terminal region of βB2-crystallin reduced the activity but did not eliminate the protein-protein interaction completely [63]. The distortion of Gln-70 in the N-terminal region, however, induces the disruption of the more compact C-terminal domain [64]. Moreover, the mutations of two adjacent residues in the last strand of βB2-crystallin Greek-key motif 4 might lead to congenital nuclear cataract via quite dissimilar mechanisms: V187M loosened the C-terminal domain hydrophobic core, V187E was a Greek-key motif breaker, while R188H perturbed the oligomeric equilibrium [65].

Acknowledgments

I thank Professor Case D for providing me the Amber12 package.

References

[1] McCammon JA (1984). Protein dynamics. Rep Prog Phys 47: 1-46.

[2] Ma J (2005). Usefulness and limitations of normal mode analysis in modeling dynamics of biomolecular complexes. Structure 13: 373–380.

[3] Bahar I, Lezon TR, Bakan A, and Shrivastava IH (2010). Normal mode analysis of biomolecular structures: functional mechanisms of membrane proteins. Chem Rev. 110: 1463-97.

[4] Kitao A and Go N (1999). Investigating protein dynamics in collective coordinate space. Curr Opin Struc Biol 9: 164-l 69.

[5] Delarue M and Dumas P (2004). On the use of low-frequency normal modes to enforce collective movements in refining macromolecular structural models. PNAS 101: 6957–6962.

[6] Bassnett S, Shi Y and Vrensen GFJM (2011). Biological glass: structural determinants of eye lens transparency. Phil. Trans. R. Soc. B 366, 1250–1264.

[7] Pierscionek B and Augusteyn RC (1988). Protein distribution patterns in concentric layers from single bovine lenses: changes with development and ageing. Curr Eye Res 7: 11-23.

[8] van Rens GLM, Driessen HPC, Nalini V, Slingsby C, de Jong WW, Bloemendal H (1991). Isolation and characterization of the cDNAs of the last two acidic β-crystallins, βA2 and βA4: Heterologous interaction in the predicted βA4-βB2 heterodimer. Gene 102:179-188.

[9] Bindels JG, Koppers A, and Hoenders HJ (1981). Structural aspects of bovine β-crystallins: Physical characterization including dissociation-association behavior. Exp Eye Res 33: 333-343.

[10] Driessen, H. P. C., He Liu BF, Liang JJ (2007). Protein-protein interactions among human lens acidic and basic beta-crystallins. FEBS Lett. 581: 3936-42.

[11] Liu B-F and Liang J J-N (2006). Domain interaction sites of human lens βB2-crystallin. J Biol Chem 281: 26-24- 2630.

[12] Bax B, Lapatto R, Nalini V, Driessen H, Lindley PF, Mahadevan D, Blundell TL, and Slingsby C (1990). X-ray analysis of βB2-Crystallin and evolution of oligomeric lens proteins. Nature 347: 776−780.

[13] Nalini V, Bax B, Driessen H, Moss DS, Lindley PF, and Slingsby C (1994). Close packing of an oligomeric eye lens beta-crystallin induces loss of symmetry and ordering of sequence extensions. J Mol Biol 236: 1250−1258.

[14] Berbers, GA. M., Boerman, 0. C., Bloemendal H, and de Jong, WW (1982). Primary gene products of bovine β-crystallin and reassociation behavior of its aggregates. Eur J Biochem 128: 495-502.

[15] Kroone RC, Elliott GS, Ferszt A, Slingsby C, Lubsen NH and Schoenmakers JGG (1994). The role of the sequence extensions in β–crystallin assembly. Protein Eng 7: 1395–1399.

[16] Trinkl S, Glockshuber R and Jaenicke R (1994). Dimerisation of βB2-crystallin: The role of the linker peptide and the N– and C-terminal extensions. Protein Sci. 3: 1392–1400.

[17] Zhang J, Li J, Huang C, Xue L, Peng Y, Fu Q, Gao L, Zhang J, Li W(2008). Targeted knockout of the mouse βB2-crystallin gene (Crybb2) induces age-related cataract. Invest Ophthalmol Vis Sci. 49: 5476-83.

[18] Skjaerven L, Hollup SM, and Reuter N (2009). Normal mode analysis for proteins. J Mol Str: THEOCHEM 898 (2009) 42–48.

[19] Noguti, T and Gō, N (1989). Structural basis of hierarchical multiple substrates of a protein. IV: rearrangements in atom packing and local determinations. Proteins 5: 125-131.

[20] Hayward, S, Kitao, A, and Gō, N (1995). Harmonicity and anharmonicity in protein dynamics: a normal mode analysis and principal component analysis. Proteins 23: 177-186.

[21] Ma J (2004). New advances in normal mode analysis of supermolecular complexes and applications to structural refinement. Curr Prot Pept Sci 5: 119–123

[22] Bahar I, Rader AJ (2005). Coarse-grained normal mode analysis in structural biology. Curr Opin Struct Biol 15: 586–592.

[23] Atilgan AR, Durell SR, Jernigan RL, Demirel MC, Keskin O, Bahar I (2001). Anisotropy of fluctuation dynamics of proteins with an elastic network model. Biophys J 80: 505–515.

[24] Tirion MM (1996). Large amplitude elastic motions in proteins from a single-parameter, atomic analysis. Phys Rev Lett. 77: 1905-1908.

[25] Eyal E, Chennubhotla C, Yang L-W, and Bahar I (2007). Anisotropic fluctuations of amino acids in protein structures: insights from X-ray crystallography and elastic network models. Bioinformatics 23: i175-i184.

[26] Isin B, Doruker P, and Bahar I (2002).Functional Motions of Influenza Virus Hemagglutinin: A Structure-Based Analytical Approach. Biophys J 82: 569–581.

[27] Hung A, Tai K, and Sansom MSP (2005). Molecular dynamics simulation of the M2 helices within the nicotinic acetylcholine receptor transmembrane domain: structure and collective motions, Biophys J 88: 3321–3333.

[28] Deriu MA, Soncini M, Orsi M, Patel M, Essex JW, Montevecchi FM, Redaelli A (2010). Anisotropic elastic network modeling of entire microtubules. Biophys J 99: 2190–2199.

[29] Bakan A, and Bahar I (2011). Computational generation inhibitor-bound conformers of p38 MAP kinase and comparison with experiments. Pacific Symposium on Biocomputing: 181-192.

[30] Stoyanova R, Brown TR (2001). NMR spectral quantitation by principal component analysis. NMR Biomed 14: 271-7.

[31] Ramadan Z, Jacobs D, Grigorov M, Kochhar S (2006). Metabolic profiling using principal component analysis, discriminant partial least squares, and genetic algorithms. Talanta 68: 1683–1691.

[32] Gendoo DMA and Harrison PM (2012). The landscape of the prion protein's structural response to mutation revealed by principal component analysis of multiple NMR ensembles. PLoS Comput Biol 8: e1002646

[33] Salomon-Ferrer R, Case DA and Walker RC (2013). An overview of the Amber biomolecular simulation package. WIREs Comput Mol Sci 3: 198-210.

[34] Essmann, U., Perera, L., Berkowitz, M.L., Darden, T., Lee, H., and Pedersen, L.G. (1995). A smooth particle mesh Ewald method. J. Chem. Phys. 103: 8577–8593.

[35] Ryckaert, J.P., Ciccotti, G., and Berendsen, H.J.C. (1977). Numerical integration of the Cartesian equations of motion of a system with constraints: Molecular dynamics of n-alkanes. J. Comput. Phys. 23: 327–341.

[36] Berendsen, H. J. C., Postma, J. P. M., van Gunsteren,W. F., DiNola, A., Haak, J. R. (1984). Molecular dynamics with coupling to an external bath. J Chem Phys 81, 3684–3690.

[37] Amadei A, Linssen AB, Berendsen HJ (1993). Essential dynamics of proteins. Proteins 17: 412–425.

[38] Teodoro ML, Phillips GN Jr, and Kavraki LE (2003). Understanding protein flexibility through dimensionality reduction. J. Comput. Biol 10: 617–634.

[39] Eyal E, Yang LW, and Bahar I (2006). Anisotropic network model: systematic evaluation and a new web interface. Bioinformatics 22: 2619-27

[40] Lee RA, Razaz M, Hayward S (2003). The DynDom database of protein domain motions. Bioinformatics 19: 1290-1291.

[41] Krissinel E and Henrick K (2007). Inference of macromolecular assemblies from crystalline state. J Mol Biol 372: 774-797.

[42] Raman B, Ramakrishna T, and Rao CM (1995). Temperature dependent chaperone-like activity of alpha-crystallin. FEBS Lett 365: 133-6.

[43] Das BK, Liang JJ, Chakrabarti B (1997). Heat-induced conformational change and increased chaperone activity of lens alpha-crystallin. Curr Eye Res 16: 303-309.

[44] del Valle LJ, Escribano C, Pe´rez JJ, Garriga P (2002). Calcium-induced decrease of the thermal stability and chaperone activity of a-crystallin. Bioch Biophys Acta 1601: 100– 109.

[45] Beebe DC, Holekamp NM, Shui Y-B (2010). Oxidative damage and the prevention of age-related cataracts. Ophthalmic Res 44:155–165.

[46] Lampi KJ, Wilmarth PA, Murray MR, and David LL (2014). Lens β-crystallins: The role of deamidation and related modifications in aging and cataract. Prog Biophys Mol Biol 115: 21-31.

[47] Moreau KL and King JA (2012). Cataract-causing defect of a mutant γ-crystallin proceeds through an aggregation pathway which bypasses recognition by the α-Crystallin Chaperone. PLoS ONE 7(5): e37256.

[48] Tama F. (2003). Normal mode analysis with simplified models to investigate the global dynamics of biological systems. Prot Pept Lett 10: 119-32.

[49] Su JG, Xu XJ, Li CH, Chen WZ, and Wang CX (2011). An analysis of the influence of protein intrinsic dynamical properties on its thermal unfolding behavior. J Biomol Struct Dyn. 29:105-21.

[50] Skliros A, Zimmermann MT, Chakraborty D, Saraswathi S, Katebi AR, Leelananda SP, Kloczkowski A and Jernigan RL (2012). The importance of slow motions for protein functional loops. Phys Biol 9: 014001.

[51] Lapatto R, Nalini V, Bax B, Driessen H, Lindley PF, Blundell TL, and Slingsby C (1991). High resolution structure of an oligomeric eye lens β-crystallin. Loops, arches, linkers and interfaces in βB2 dimer compared to monomeric γ-crystallin. J Mol Biol 222: 1067-1083.

[52] Norledge BV, Trinkl S, Jaenicke R and Slingsby (1997). The x-ray structure of a mutant eye lens βB2-crystallin with truncated sequence extensions. Protein Sci 6: 1612-1620.

[53] MacDonald JT, Purkiss AG, Smith MA, Evans P, Goodfellow JM, and Slingsby C (2005). Unfolding crystallins: the destabilizing role of a beta-hairpin cysteine in betaB2-crystallin by simulation and experiment. Protein Sci 14: 1282-92.

[54] Evans P, Slingsby C, and Wallace BA (2008). Association of partially folded lens betaB2-crystallins with the alpha-crystallin molecular chaperone. Biochem J 409: 691-699

[55] Lampi KJ, Fox CB, David LL (2012). Changes in solvent accessibility of wild-type and deamidated βB2-crystallin following complex formation with αA-crystallin. Exp Eye Res 104: 48-58.

[56] Lange OF and Grubmüller H (2006). Can principal component yield a dimension reduced description of protein dynamics on long time scale? J Phy Chem B 110: 22842-22852.

[57] Skjaerven L, Martinez A, and Reuter N. (2011). Principal component and normal mode analysis of proteins; a quantitative comparison using the GroEL subunit. Proteins 79: 232-243.

[58] Luo J and Bruice TC (2007). Low-frequency normal modes in horse liver alcohol dehydrogenase and motions of residues involved in the enzymatic reaction. Biophys Chem 126: 80–85.

[59] Adamovic I, Mijailovich SM, and Karplus M (2008). The elastic properties of the structurally characterized myosin II S2 subdomain: A molecular dynamics and normal mode analysis. Biophys J 94: 3779–3789

[60] Vemparala S, Mehrotra S, Balaram H (2011). Role of loop dynamics in thermal stability of mesophilic and thermophilic adenylosuccinate synthetase: A molecular dynamics and normal mode analysis study. Biochim Biophys Acta 1814: 630–637.

[61] Lu M and Ma J (2005) The role of shape in determining molecular motions. Biophysical Journal 89: 2395–2401.

[62] Fenwick RB, Orellana L, Esteban-Martín S, Orozco M, Salvatella X (2014). Correlated motions are a fundamental property of β-sheets. Nat. Commun. 5: 4070-

[63] Liu B-F, Liang J J-N (2005). Interaction and biophysical properties of human lens Q155* βB2-crystallin mutant. Mol Vis 11: 321-327.

[64] Takata T, Smith JP, Arbogast B, David LL, and Lampi KJ (2010). Solvent accessibility of betaB2-crystallin and local structural changes due to deamidation at the dimer interface. Exp Eye Res 91: 336-346.

[65] Zhang K, Zhao W-J, Leng XY, Wang SY, Yao K, Yan YB (2014). The importance of the last strand at the C-terminus in beta B2-crystallin stability and assembly. Biochim Biophys Acta. 1842: 44-55.